AIP | Review of Scientific Instruments

Cancellation of environmental effects in resonant mass sensors based on resonance mode and effective mass

Kianoush Naeli and Oliver Brand

Citation: Rev. Sci. Instrum. **80**, 063903 (2009); doi: 10.1063/1.3143567
View online: http://dx.doi.org/10.1063/1.3143567
View Table of Contents: http://rsi.aip.org/resource/1/RSINAK/v80/i6
Published by the American Institute of Physics.

Cancellation of environmental effects in resonant mass sensors based on resonance mode and effective mass

Kianoush Naeli[a] and Oliver Brand
School of Electrical and Computer Engineering, Georgia Institute of Technology, Atlanta, Georgia 30332-0250, USA

(Received 16 July 2008; accepted 6 May 2009; published online 5 June 2009)

A novel technique is developed to cancel the effect of environmental parameters, e.g., temperature and humidity, in resonant mass sensing. Utilizing a single resonator, the environmental cancellation is achieved by monitoring a pair of resonant overtones and the effective sensed mass in those overtones. As an eminent advantage, especially compared to dual-mode temperature compensation techniques, the presented technique eliminates any need for previously measured look-up tables or fitting the measurement data. We show that a resonant cantilever beam is an appropriate platform for applying this technique, and derive an analytical expression to relate the actual and effective sensed masses on a cantilever beam. Thereby, it is shown that in applying the presented technique successfully, the effective sensed masses must not be the same in the investigated pair of resonance overtones. To prove the feasibility of the proposed technique, flexural resonance frequencies of a silicon cantilever are measured before and after loading with a strip of photoresist. Applying the presented technique shows significant reductions in influence of environmental parameters, with the temperature and humidity coefficients of frequency being improved from -19.5 to 0.2 ppm $^{\circ}C^{-1}$ and from 0.7 to -0.03 ppm $\%RH^{-1}$, respectively. © *2009 American Institute of Physics.*
[DOI: 10.1063/1.3143567]

I. INTRODUCTION

Mass sensing with a resonant sensor was first demonstrated using quartz crystal microbalances,[1] and is based on the concept that a change in the resonant sensor's mass causes a change in the resonance frequency.[2] Facilitated by the development of microfabrication technologies, this method has been successfully implemented in other bulk acoustic wave resonators,[3] as well as in surface acoustic wave sensors[4] and resonant cantilevers.[5–9] If these sensors are used for (bio-)chemical detection, the mass change is typically due to adsorption or absorption of target analytes to a sensitive layer coating the resonator.

A major challenge in resonant mass sensing is to distinguish between frequency variations caused by a mass change and frequency variations caused by environmental changes, e.g., temperature, viscosity, or humidity. In other words, it is ultimately desirable for a resonant mass sensor to increase the frequency change caused by a mass change, while eliminating the frequency drifts caused by ambient condition variations. However, it is known that a temperature change causes variations in the resonator's elastic modulus and/or dimensions,[10] which reflect as a resonance frequency change. On the other hand, changes in the ambient humidity and viscosity can alter the viscous damping of the resonant system and cause resonance frequency drift.[10–12]

To compensate for frequency drifts caused by ambient variations, temperature fluctuations in particular, one of the widely investigated approaches is to utilize another resonator as a reference.[13–15] In this approach, the sensing resonator, which is coated with the sensitive layer, and the uncoated reference resonator operate under the same environmental conditions. Under the assumption that any environmental parameter affecting the resonance behavior will cause the same frequency drift in both sensing and reference resonators, the induced frequency change by an added mass can be extracted by subtracting the frequency changes in the two resonators. The drawback of this method originates from the above assumption that both resonators have exactly the same mechanical properties or at least respond similarly to environmental changes. In practice, however, no two resonators have exactly identical mechanical properties, even if they are fabricated in the same batch process; consequently, their resonance frequencies and their responses to varying environmental parameters may not be same. Overall, this approach can be helpful in estimating the frequency change by a mass-uptake, but it cannot provide a complete solution.

Several other approaches in minimizing the temperature-induced resonance frequency drift include active frequency control with a cointegrated temperature sensor[13,16] or feedback loop,[17] passive temperature compensation using the stress induced by thin films,[18–20] and selection of structural materials that are less sensitive to temperature.[21] When using a cointegrated temperature sensor, it is mandatory to establish a reproducible relationship between temperature and the resonance frequency change. Here, a major challenge is that the temperature coefficient of the resonance frequency varies from one resonator to another, thus requiring calibration of each sensor. Also, the required circuitry for precise sensing

[a]Tel.: +1-404-894-9425. FAX: +1-404-894-4700. Electronic mail: kianoush@gatech.edu.

of temperature may increase the complexity and cost of the overall sensing system. Finally, this approach only compensates the temperature effect, but leaves other contributing effects, e.g., humidity, uncompensated. On the other hand, passive approaches utilizing thin-film-induced stresses are highly dependent on the packaging, the adopted resonant structure, and the quality of the selected thin film. Finally, finding an absolutely temperature insensitive material is not a trivial task, and integrating such material with existing microfabrication technologies includes challenges, both in terms of feasibility and cost.

Another approach in compensating the temperature effect is to study the variation of different resonance modes[22–24] or overtones.[25] Here, a relationship between temperature and the frequency change for different overtones or modes is established; hence, the same resonant mass sensor also acts as a thermometer. For such a sensor, with the help of a look-up table or calibrated coefficients, temperature-induced frequency changes can be eliminated. Nevertheless, the main drawback of this approach is the need for such look-up tables or coefficients.

In this paper, we describe a technique for canceling the effect of environmental parameters in resonant mass sensing based on monitoring the overtones[26] of partially coated resonators. Like the aforementioned mode-based compensation approaches, an essential part of this technique is also based on comparing the frequency drifts of different overtones. However, as an eminent advantage, this technique eliminates any need for premeasured temperature-frequency look-up tables. In fact, the aim of the presented technique is to cancel any environment-related frequency drift only by the aid of a single resonator. The applicability of the presented technique is tested on a cantilever resonating in flexural modes, with the results showing excellent agreement with the theoretical predictions.

II. THEORY

In this section, first the frequency dependence on variations in mass and environmental parameters is described. Next, a special class of resonators is identified, whose normalized frequency change caused by environmental parameters is independent of the resonance overtone. The technique presented in this paper is aimed at such resonators.

For all mechanical resonators, according to Rayleigh's quotient method,[27,28] the resonance frequency f is determined by the ratio of the potential energy U and the inertial part of the kinetic energy KE_I

$$f = \frac{1}{2\pi}\sqrt{\frac{U}{\mathrm{KE}_I}}, \tag{1}$$

where KE_I is expressed by the kinetic energy (KE) as follows:

$$\mathrm{KE}_I = \frac{\mathrm{KE}}{(2\pi f)^2}.$$

Therefore, variations in KE_I and U will reflect as a change of the resonance frequency Δf, which for small variations is calculated as

$$\frac{\Delta f}{f} = -\frac{1}{2}\left(\frac{\Delta \mathrm{KE}_I}{\mathrm{KE}_I} - \frac{\Delta U}{U}\right). \tag{2}$$

For a mass-spring system, whenever variations of the vibration amplitude can be neglected, Eq. (2) simplifies to

$$\frac{\Delta f}{f} = -\frac{1}{2}\left(\frac{\Delta m^*}{m^*} - \frac{\Delta k^*}{k^*}\right), \tag{3}$$

where m^* and k^* are the effective mass and spring constant, respectively. In a resonant mass sensor used for (bio-)chemical sensing, the detection is accomplished by binding of target molecules to the surface of the resonator,[29,30] which results in an effective mass change Δm^*. As long as the effect of the added mass on the potential energy can be neglected, i.e., k^* does not change with Δm^*, the change of the resonance frequency can be described as a function of the independent parameter mass m and also environmental parameters, e.g., temperature T, relative humidity (RH), etc.,

$$\frac{\Delta f}{f} = \frac{\Delta f(m)}{f} + \frac{\Delta f(T,\mathrm{RH},\mathrm{etc.})}{f}, \tag{4}$$

and with respect to Eq. (3)

$$\frac{\Delta f}{f} = -\frac{1}{2}\frac{\Delta m^*}{m^*} + \frac{\Delta f(T,\mathrm{RH},\mathrm{etc.})}{f}. \tag{5}$$

The second term in Eq. (5) emerges because of variation in the potential energy, i.e., the effective spring constant, with environmental parameters. Without mass change, the resonance frequency variation will only depend on environmental parameters. The influence of these parameters on the resonance frequency is caused by changes in the resonator's material properties and/or geometry. In general, for a resonator, the normalized frequency changes of overtones due to environmental changes are not identical; however, in a special class of resonators (e.g., homogeneous cantilever beams resonating in the flexural modes) the overtone frequencies are related to each other through constant coefficients. In these resonators, the resonance frequency f_i of the ith overtone is described as

$$f_i = \lambda_i^2 \mathbf{F}(E,\rho,l_{x,y,z}), \tag{6}$$

where λ_i is the overtone constant (i.e., the resonance mode eigenvalue) and $\mathbf{F}$ is a function of the resonator geometry $l_{x,y,z}$, and the material properties, i.e., Young's modulus E, Poisson ratio ν, and density ρ. For this class of resonators, in case of environmental variations, the change in the resonator geometry and material properties will be same for all overtones; therefore, the change in $\mathbf{F}$ will be same for all overtones. Hence, the resonance frequency change Δf_i of the ith overtone can be described as

$$\Delta f_i = \lambda_i^2 \Delta \mathbf{F}, \tag{7}$$

where $\Delta \mathbf{F}$ is a change in $\mathbf{F}$, which is independent of resonance overtone. Combining Eqs. (6) and (7), for all overtones, the relative frequency change $\Delta f_i/f_i$ becomes independent of the overtone constant λ_i

$$\frac{\Delta f_i}{f_i} = \frac{\Delta \mathbf{F}}{\mathbf{F}}. \tag{8}$$

Since all variables affecting $\mathbf{F}$ are in fact functions of environmental parameters, Eq. (8) can be rewritten with respect to Eq. (5)

$$\frac{\Delta f_i(T,\mathrm{RH},\mathrm{etc.})}{f_i} = \frac{\Delta \mathbf{F}(T,\mathrm{RH},\mathrm{etc.})}{\mathbf{F}}. \tag{9}$$

To completely describe Eq. (5) for a given overtone frequency, the effect of any added mass in that overtone needs to be included. In a resonant mass sensor, the attached analyte mass Δm generally vibrates with different normalized amplitudes in different overtones, and thus its contributed effective mass Δm^* will be different in those overtones. In other words, if the actual mass change is Δm the effective mass change in the ith overtone is given by

$$\Delta m_i^* = \alpha_i \Delta m, \tag{10a}$$

where α_i is the effective mass coefficient and calculated only based on the mode-shape and the location of the added mass on the resonator surface. Likewise, the total effective mass of the resonator can also be described based on its actual mass and the resonance overtone by a coefficient β_i

$$m_i^* = \beta_i m. \tag{10b}$$

By applying Eqs. (9) and (10) to Eq. (5), the normalized frequency change of the ith overtone $\Delta f_i/f_i$ is given by

$$\frac{\Delta f_i}{f_i} = -\frac{1}{2}\frac{\alpha_i}{\beta_i}\frac{\Delta m}{m} + \frac{\Delta \mathbf{F}(T,\mathrm{RH},\mathrm{etc.})}{\mathbf{F}}. \tag{11}$$

Hence, by subtracting the normalized frequencies of two overtones i and j, it is possible to eliminate the effect of environmental parameter variations

$$\frac{\Delta f_i}{f_i} - \frac{\Delta f_j}{f_j} = -\frac{1}{2}\left(\frac{\alpha_i}{\beta_i} - \frac{\alpha_j}{\beta_j}\right)\frac{\Delta m}{m}, \tag{12a}$$

If the resonator has the same effective mass in all overtones, i.e., $\beta_i = \beta_j$, Eq. (12a) simplifies to

$$\frac{\Delta f_i}{f_i} - \frac{\Delta f_j}{f_j} = -\frac{1}{2}(\alpha_i - \alpha_j)\frac{\Delta m}{m^*}. \tag{12b}$$

As mentioned earlier, the conditions for establishing Eqs. (12a) and (12b) are: (1) the added mass must not change the potential energy of the system (i.e., no change in the resonator effective stiffness), and (2) the effective added mass must be different in the investigated overtones (i.e., $\alpha_i \neq \alpha_j$); otherwise the difference of the relative frequency changes in Eq. (12b) will be always zero.

A. Beam resonators in flexural modes

Beams in flexural resonance modes are prominent examples of the resonators that fit the conditions described for Eqs. (12a) and (12b). For homogenous, clamped-free (i.e., cantilever) or clamped-clamped beams, when damping of the resonant system is negligible, f_i can be described as[27]

$$f_i = \lambda_i^2 \frac{1}{2\pi\sqrt{12}}\frac{h}{L^2}\sqrt{\frac{E}{\rho}}, \tag{13}$$

where L and h are the beam length and thickness, respectively. Comparing to Eq. (6), and considering the discussion for Eq. (9), the frequency function $\mathbf{F}$ of a beam in a flexural mode (overtone) becomes

$$\mathbf{F}(E,\rho,l_{x,y,z}) = \mathbf{F}(T,\mathrm{RH},\mathrm{etc.}) = \frac{1}{2\pi\sqrt{12}}\frac{h}{L^2}\sqrt{\frac{E}{\rho}}. \tag{14}$$

In the remainder of this paper our focus will be on such cantilever beams in flexural resonance modes. To calculate the effective mass of a deposited layer on the cantilever surface, the resonator's KE is explored. The maximum KE of a thin homogenous cantilever beam with a uniform cross section is given by[27]

$$\mathrm{KE} = \frac{1}{2}\omega^2 \frac{m}{L}\int_0^L y^2(x)dx, \tag{15}$$

where y is the vibration amplitude at a point x along the beam, and m and ω are the beam actual mass and angular velocity, respectively. A particle with mass dm, which is attached at point x on the cantilever surface, increases the KE by dKE

$$d\mathrm{KE} = \frac{\omega^2}{2}y^2(x)dm, \tag{16}$$

provided that the change in the resonance amplitude is negligible. If the attached particle does not contribute to the stiffness of the beam, i.e., to the potential energy, the principle of energy conservation requires the same KE before and after attachment, i.e.,

$$\frac{1}{2}\omega_f^2 \frac{m}{L}\int_0^L y^2(x)dx + \frac{\omega_f^2}{2}y^2(x)dm = \frac{1}{2}\omega_i^2 \frac{m}{L}\int_0^L y^2(x)dx, \tag{17}$$

where ω_i and ω_f are the angular velocities for the initial case (without dm attached) and final case (with dm attached). Since for all flexural modes of a resonating cantilever beam the integral value of Eq. (15) is equal to $1/4Ly^2(L)$,[31,32] Eq. (17) can be rearranged as

$$dm\omega_f^2 y^2(x) = \tfrac{1}{4}m(\omega_i^2 - \omega_f^2)y^2(L). \tag{18}$$

Assuming ω_i and ω_f are almost identical, the resulting relative frequency change $d\omega/\omega$ due to the added mass dm at distance x is obtained as

$$\frac{d\omega}{\omega} = \frac{\omega_f - \omega_i}{\omega_i} = -\frac{1}{2}\frac{dm}{\frac{1}{4}m}\frac{y^2(x)}{y^2(L)}. \tag{19}$$

On the other hand, using Eq. (15), the effective mass of the cantilever m^* can be conceived as a lumped mass placed on a point that has the maximum vibration amplitude, i.e., on the cantilever tip with vibration amplitude $y(L)$

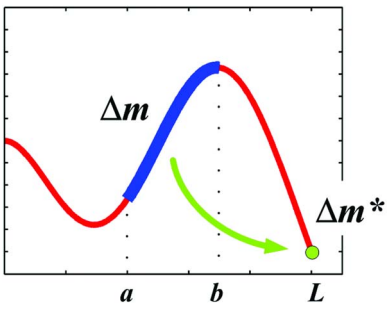

FIG. 1. (Color online) Schematic of the third overtone mode-shape of a cantilever; Δm, the mass of the added layer, represented with a thicker line, can be considered as a lumped effective mass Δm^* on the cantilever tip.

$$\frac{1}{2}\omega^2 m^* y^2(L) = \frac{1}{2}\omega^2 \frac{m}{L}\int_0^L y^2(x)dx. \tag{20}$$

Therefore, after applying the integral value $1/4Ly^2(L)$, the effective mass placed on the cantilever tip is for all overtones[33]

$$m^* = \tfrac{1}{4}m. \tag{21}$$

Thus Eq. (19) becomes

$$\frac{d\omega}{\omega} = -\frac{1}{2}\frac{dm}{m^*}\left[\frac{y(x)}{y(L)}\right]^2. \tag{22}$$

The result of Eq. (22) is consistent with the reported experimental results by Dohn *et al.*,[34,35] indicating the influence of the added particle location on the induced frequency change. With the same argument, the frequency change due to attachment of a continuous sequence of discrete particles, e.g., deposition of a layer or sorption of target molecules into a sensitive film on the surface of the resonator, can be described as

$$\frac{d\omega}{\omega} = -\frac{1}{2m^*}\int_a^b \left[\frac{y(x)}{y(L)}\right]^2 dm, \tag{23}$$

where a and b are the starting and ending points of the layer coverage, respectively. Assuming a uniform mass loading between a and b with a total added mass Δm, Eq. (23) simplifies to

$$\frac{d\omega}{\omega} = -\frac{\Delta m}{2m^*}\frac{1}{b-a}\int_a^b \left[\frac{y(x)}{y(L)}\right]^2 dx. \tag{24}$$

Hence, comparing to Eq. (11), the effective mass coefficient α_i in the ith overtone is

$$\alpha_i = \frac{1}{(b-a)y^2(L)}\int_a^b y^2(x)dx. \tag{25}$$

Here, $\Delta m^* = \alpha_i \Delta m$ is the effective mass of the added mass when considered as a lumped point mass on the beam tip (see Fig. 1). It is important to note that when the added layer covers the entire cantilever, according to Eq. (25), α_i will have the same value of $1/4$ for all flexural modes. Hence, to have a successful cancellation of the effect of environmental parameters through Eqs. (12a) and (12b), the attached layer must only partially cover the cantilever surface (i.e., $\alpha_i \neq \alpha_j$).

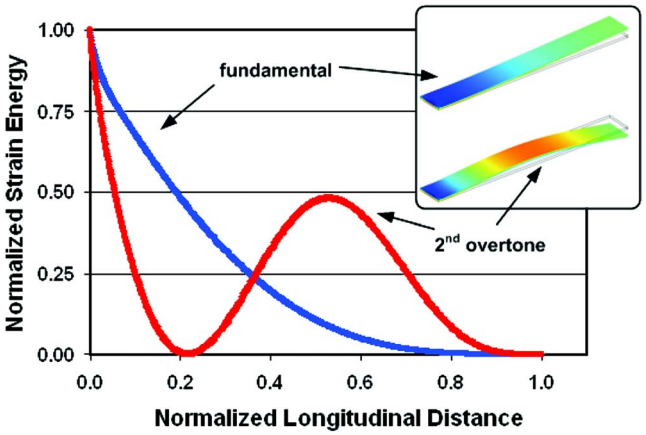

FIG. 2. (Color online) FEM simulation results for the longitudinal distributions of the normalized strain energy in a cantilever beam for the fundamental and second flexural resonance modes; also for these vibration modes, the normal stress distributions are shown in the inset.

B. Technical considerations

To apply the presented technique in a resonant cantilever mass sensor, the detection must be accomplished through interaction (binding) of target analyte with a sensitive layer that partially covers the resonator surface. If the layer is uniformly deposited, it is a fair assumption that binding also takes place with a uniform rate across the layer. There are always at least two different flexural modes (overtones) of the resonant cantilever that exhibit different effective mass coefficients for a partially covering layer. Therefore, the first requirement in applying Eqs. (12a) and (12b), i.e., having different α_i in different overtones, can be satisfied. However, addressing the second requirement, i.e., maintaining the same stiffness after binding, depends on the type of material or the location of binding on the cantilever surface. In other words, either the binding must have a negligible effect on the stiffness of the sensing layer, or the sensing layer must be placed at a location that causes a minimal contribution to the strain energy of the desired overtones. Such locations include areas on the cantilever surface that experience minimal stress in a flexural resonance mode. Results of finite element simulations presented in Fig. 2 indicate that in case of the fundamental and the second flexural modes, the last 20% along a cantilever length satisfy the second requirement. In general, by approaching the cantilever tip, the contribution of the sensing layer on the stress decreases; but at the same time, the difference in the values of the effective mass coefficients for any two overtones starts diminishing, therefore, the difference of the relative frequency changes in Eqs. (12a) and (12b) becomes smaller.

III. EXPERIMENTS

Flexural resonance frequencies of a silicon cantilever with length, width, and thickness of 1050, 130, and 11 μm, respectively, were investigated. The surface of the cantilever was covered with 0.8 μm silicon dioxide. The resonator vibration in air was electromagnetically exited by passing an alternating current along the perimeter of cantilever in the presence of a static magnetic field of 0.2 T. The transverse

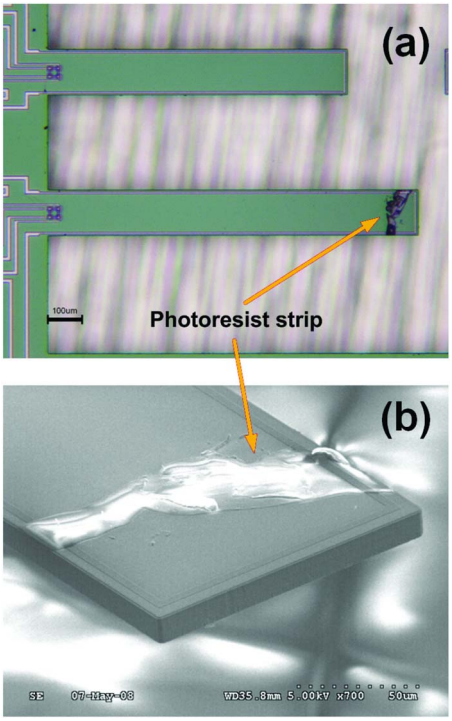

FIG. 3. (Color online) (a) Optical micrograph of magnetically excitable resonant cantilevers. The cantilever tested in this work (the bottom cantilever) is covered by a strip of photoresist about 90 μm from the tip. (b) SEM picture of the photoresist strip near the cantilever tip.

beam vibrations were sensed on chip by a piezoresistive Wheatstone bridge located at the clamped-end of the beam. The amplitude/phase transfer characteristics of the resonator were recorded by an Agilent Network Analyzer 4395A. Each data point presented in this work is an average of at least five repeated measurements, with a maximum standard deviation of 10 ppm. To improve the accuracy of the extracted resonance frequency, the measured transfer characteristic around each peak was fitted to the resonance curve of a simple harmonic oscillator.[36] The ambient temperature and humidity were controlled with an ESPEC SH-241 environmental chamber, with a resolution of 0.1 °C in temperature, and 1% in RH.

The effect of mass loading was investigated by depositing a strip of SC1813 photoresist at approximately 90 μm from the cantilever free-end (Fig. 3). For this location, according to Eq. (25), the effective mass coefficient α_1 is approximately 0.8. To evaporate the photoresist solvent, the sample was baked for 45 min at 100 °C in the oven. Although identifying the photoresist mass has no influence in evaluating the validity of the presented technique in cancellation of environmental parameters, the approximate mass of the photoresist layer was calculated by examining the frequency change at a constant temperature.[35] At 10 °C and for the fundamental flexural mode with $\alpha_1=0.8$, according to Eqs. (24) and (21), the actual added photoresist mass is calculated as 0.095% of the actual cantilever mass, i.e., approximately 3.6 ng.

IV. RESULTS AND DISCUSSION

In this section, first we describe the effect of environmental parameters, i.e., temperature and humidity, on the resonance frequency drift of the tested cantilever. These effects are monitored for both cases that the cantilever has been resonating with and without the added photoresist mass. Next, by calculating the difference between the measured relative resonance frequency changes in different flexural modes, i.e., using Eq. (12), the effectiveness of the proposed technique in cancellation of the temperature and humidity effects is examined. Ideally, as expressed by Eq. (12), it is expected that the calculated difference of the relative frequency changes becomes independent of environmental effects, but only depends on the added mass and the effective mass coefficients.

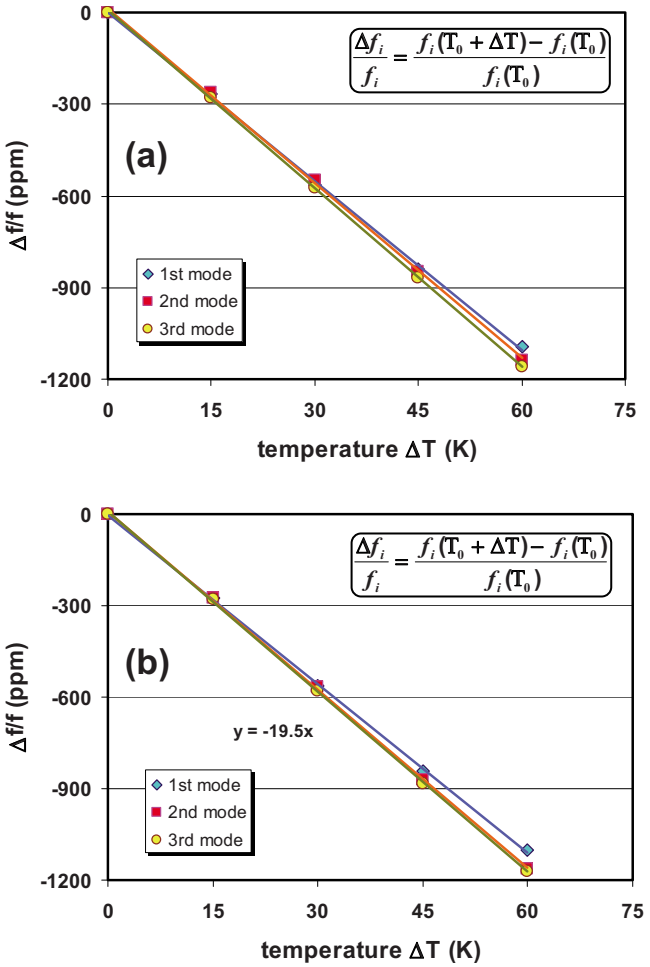

FIG. 4. (Color online) Relative frequency change $\Delta f/f$ of the first three flexural modes (fundamental, second, and third overtones) for (a) the unloaded and (b) the loaded cantilever vs temperature change ΔT (reference temperature $T_0=10$ °C).

A. Temperature effect

In the performed measurements, the initial temperature was 10 °C. The influence of temperature was studied by increasing it to 70 in 15 °C steps, while the RH was stabilized at 45% (for 25 °C and higher). The temperature stability in the measured sample was verified by monitoring the (lack of) temperature-dependent resistance variations of an extra pair of on-chip resistors. The resistance values were measured with a Keithley 2400 Sourcemeter. Figure 4 shows the relative frequency change of both the unloaded and the

TABLE I. Measured resonance frequency and quality factor for the fundamental and the next two flexural resonance modes (overtones) of the unloaded cantilever beam at 10 and 70 °C. The theoretical values of the corresponding overtone constants are indicated by λ_i.

		$T=10$ °C		$T=70$ °C	
	λ_i	f (Hz)	Q -factor	f (Hz)	Q -factor
Fundamental mode	1.875	13 532.4	360.7	13 517.6	361.0
Second overtone	4.694	84 874.3	946.5	84 777.8	999.1
Third overtone	7.855	237 467	1378	237 192	1504

loaded cantilever as a function of the temperature increment for different flexural modes (overtones); as expected from Eqs. (13) and (14), the temperature-induced relative frequency changes ($\Delta f_n/f_n=\Delta \mathbf{F}/\mathbf{F}$) are coinciding and exhibiting almost equal temperature coefficients, namely, -19.5 ppm °C^{-1} for the second overtone. These results confirm that the measured cantilever beam follows the relationship presented in Eq. (9), hence, it can be considered as a suitable example of the class of resonators identified by Eq. (6). Table I summarizes the measured absolute frequencies and quality factors of the unloaded cantilever for the investigated overtones at the initial and final temperatures (i.e., 10 and 70 °C, respectively).

The combined effects of added mass and temperature on the resonance frequency are shown in Fig. 5, which plots the relative frequency drift of each overtone as a function of the temperature change. In this figure, the observed relative frequency drift for $\Delta T=0$ °C, i.e., at the reference temperature of 10 °C, is only due to the effect of mass change. Increasing temperature affects the frequency with a similar trend, as shown in Fig. 4, and the frequency drift in each overtone follows a trend parallel to the drifts in other overtones; however, since the effective mass in each overtone is different, the plots of the relative frequency change for different overtones have different Y-intercepts. In other words, for a given temperature, the relative frequency drift of each overtone is different because the coefficients of effective mass in the investigated overtones are different.

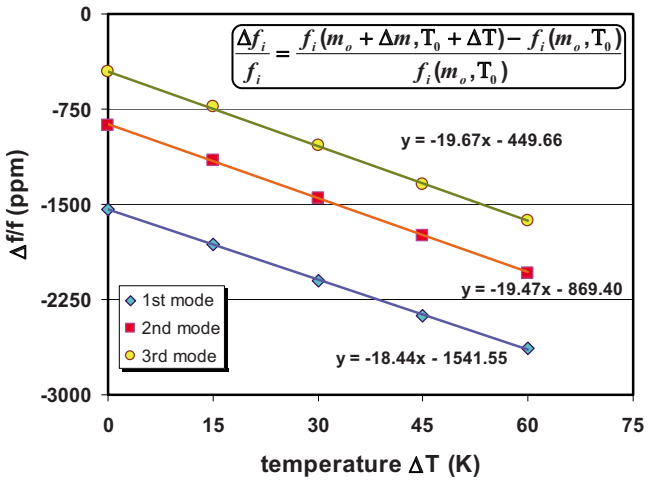

FIG. 5. (Color online) Relative frequency change $\Delta f/f$ of the first three flexural modes of cantilever as the result of a fixed mass change Δm, vs temperature change ΔT (reference temperature $T_0=10$ °C).

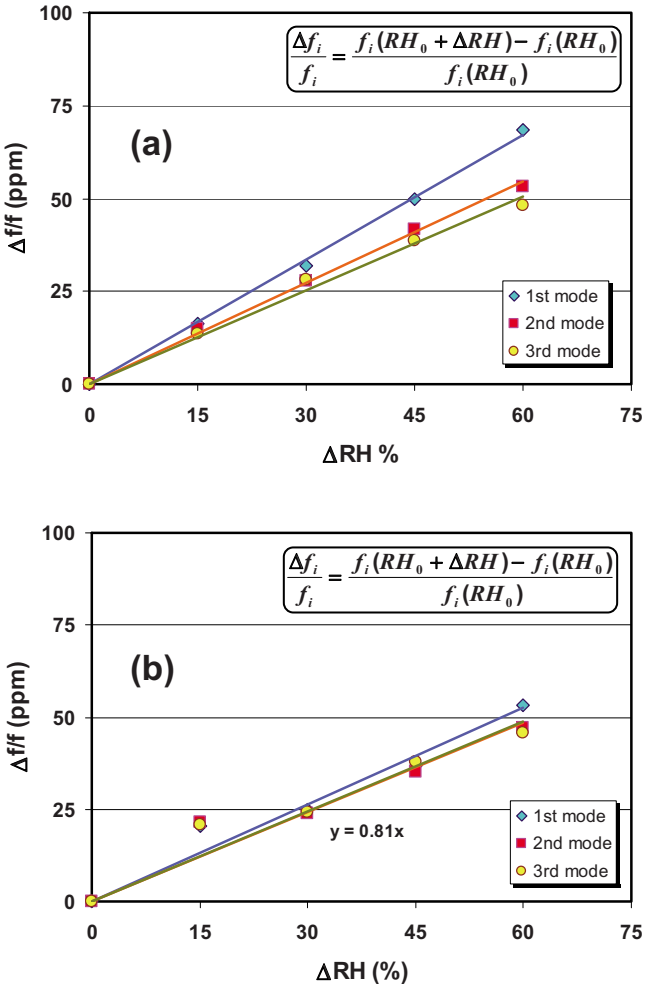

FIG. 6. (Color online) Relative frequency change $\Delta f/f$ of the flexural modes (fundamental, second, and third overtones) for (a) the unloaded and (b) the loaded cantilever versus RH change ΔRH (reference relative humidity $RH_0=30\%$).

B. Humidity effect

To investigate the effect of RH, the temperature was kept constant at 55 °C, while the RH was increased from 30% to 90% in 15% steps. For both loaded and unloaded cantilever, the effect of RH on the relative frequency drift in flexural modes is presented in Fig. 6. Similar to the argument made for temperature effects, the relative variations in flexural mode frequencies are coinciding and independent of the overtone number. Clearly, the effect of humidity is not as pronounced as the effect of temperature; for example the second flexural mode has a humidity coefficient as low as 0.8 ppm %RH^{-1}. For the loaded cantilever [Fig. 6(b)], none of the three flexural modes appears to follow the linear trend for the first 15% increment of RH; nevertheless, for both loaded and unloaded cases, all data points are coinciding. The combined effects of mass loading and RH variations in the resonance frequency are shown in Fig. 7. Similar to the temperature case (Fig. 5), for different overtones, the plots of relative frequency drifts versus RH also follow parallel

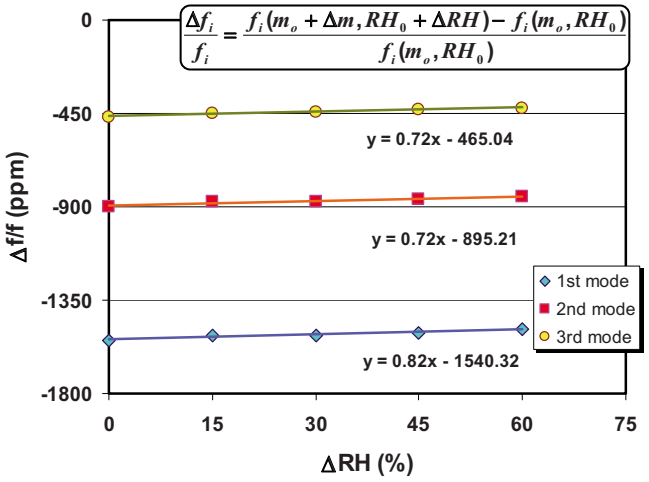

FIG. 7. (Color online) Relative frequency change $\Delta f/f$ of the first three flexural modes of cantilever as the result of a fixed mass change Δm, versus RH change ΔRH (reference relative humidity RH_0=30%).

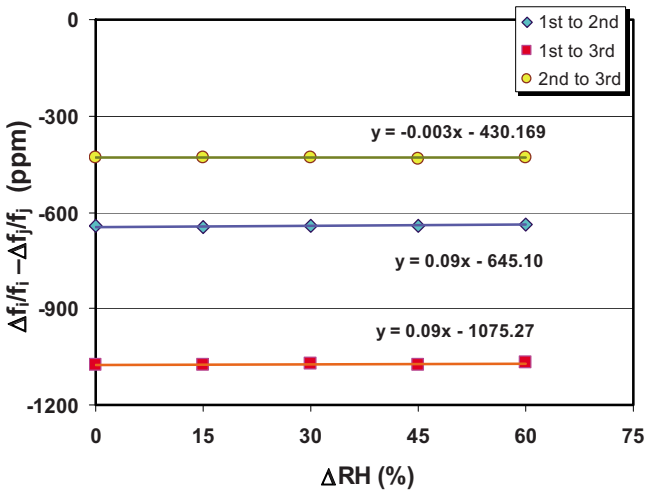

FIG. 9. (Color online) Cancellation of humidity dependence by evaluating the difference of relative frequency change $\Delta f/f$ of two overtones (based on the data from Fig. 7).

trends, but because of the dominating influence of the added mass, the slopes are more gradual, e.g., 0.7 ppm $\%RH^{-1}$ for the second flexural mode.

C. Environmental effect cancellation

As observed in Fig. 5, for a given temperature, the added mass does not have the same effect on each of the overtone frequencies, but it follows the prediction of Eq. (24). However, the variations in the relative resonance frequencies with temperature exhibit almost identical slopes. Hence, after subtracting the relative frequency changes of every two overtones according to Eq. (12b), the resulting plot, shown in Fig. 8, is almost temperature independent. For example, the temperature coefficient of the second overtone, as shown in Fig. 5, is −19.5 ppm $°C^{-1}$, but after applying Eq. (12b) to the measurement results of the second and third overtones, the temperature dependence is reduced to 0.2 ppm $°C^{-1}$, an almost two orders of magnitude improvement.

Similarly, Fig. 9 shows that the result of Eq. (12b) also cancels the effect of humidity. In this case, the humidity coefficient of the second overtone is 0.7 ppm $\%RH^{-1}$ (Fig. 7), but after applying the proposed technique to the results of the second and third overtones, the humidity dependence decreases to −0.03 ppm $\%RH^{-1}$ (see Fig. 9), literally the level of measurement error.

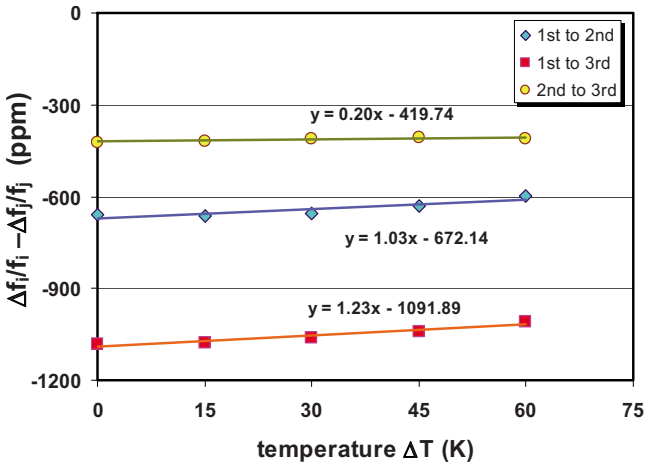

FIG. 8. (Color online) Cancellation of temperature dependence by evaluating the difference of relative frequency change $\Delta f/f$ of two overtones (based on the data from Fig. 5).

Theoretically, applying Eq. (12b) shall result in a complete cancellation of temperature effects. However, as shown in Figs. 4 and 6, the temperature coefficients of the overtones are not exactly the same, hence, the differences of the relative overtone frequency changes, shown in Figs. 8 and 9, slightly vary with the temperature. The reason for the slight difference in the temperature coefficients of the overtones can be attributed to the facts that (1) the tested cantilever (see Fig. 3) is not an ideal beam with an ideal clamped-end boundary condition; in fact, because of fabrication limits, the thickness of the cantilever slightly varies along the beam, and also, the clamped-end of the beam is not attached to a solid straight wall, but to the upper rim of an etched cavity. (2) The vibration amplitude, especially in case of the fundamental flexural mode, can exceed the small amplitude assumption used in derivation in Eq. (13); the maximum vibration amplitude of the beam was up to 35 μm. (3) The contribution of the added mass to the resonator stiffness can cause a nonideality and void the assumption made in deriving Eq. (4). Finally, (4) as presented in Table I, the resonance quality factor is not identical in different overtones; hence, the relative frequency shift due to damping is not identical either.

Ideally, since the Y-intercepts in Figs. 8 and 9 are only functions of the effective added mass, they must also have the same values for a given combination of overtones. In fact, as observed in the figures, the values of Y-intercepts are slightly different. The main reason for this variation is the fact that the reference temperatures (and RH) for the cases shown in Figs. 8 and 9 are different, thus the results show a slight deviation. The reference temperatures in Figs. 8 and 9 are 10 and 55 °C, respectively.

V. CONCLUSION

In this paper, a novel technique for cancellation of environmental effects (e.g., temperature and relative humidity) on the resonance frequency of resonant mass sensors is introduced. After applying this technique to a resonant cantilever, the undesired resonance frequency shifts caused by environmental parameters, namely, temperature and humidity, are suppressed by up to two orders of magnitude. To detect an added mass and meanwhile cancel the effect of environmental parameters, the presented technique needs only four frequency measurements; i.e., measuring the frequency of a pair of resonance overtones and comparing them with another pair measured before the potential variation in the mass. Hence, using a single sensor, this technique eliminates any need for look-up tables, or need for numerically adjusting the measurement results. The requirement in applying the presented technique are (1) the added mass must affect the examined overtone frequencies with different ratios, and (2) the added mass must not change the potential energy of the resonant system, i.e., they must have a minimal effect on the resonator stiffness. To fulfill the former requirement, the surface of resonant mass sensor, e.g., a mass-sensitive (bio-)chemical sensor, must be partially covered with the sensing layer. To address the latter requirement, either the binding induced changes in the modulus of elasticity of the sensing layer must be negligible, or the sensing layer must be deposited on areas of the resonator with minimal potential strain energy.

ACKNOWLEDGMENTS

This work has been funded in part by the National Science Foundation under Grant Nos. 0606981and 0601467.

[1] W. H. King, Anal. Chem. **36**, 1735 (1964).
[2] V. M. Mecea, Sens. Actuators, A **40**, 1 (1994).
[3] H. Zhang and E. S. Kim, J. Microelectromech. Syst. **14**, 699 (2005).
[4] H. Wohltjen, Sens. Actuators **5**, 307 (1984).
[5] V. Ferrari, D. Marioli, A. Taroni, E. Ranucci, and P. Ferruti, IEEE Trans. Ultrason. Ferroelectr. Freq. Control **43**, 601 (1996).
[6] D. Lange, C. Hagleitner, A. Hierlemann, O. Brand, and H. Baltes, Anal. Chem. **74**, 3084 (2002).
[7] F. M. Battiston, J. P. Ramseyer, H. P. Lang, M. K. Baller, C. Gerber, J. K. Gimzewski, E. Meyer, and H. J. Güntherodt, Sens. Actuators B **77**, 122 (2001).
[8] T. Thundat, P. I. Oden, and R. J. Warmack, Microscale Thermophys. Eng. **1**, 185 (1997).
[9] M. Li, H. X. Tang, and M. L. Roukes, Nat. Nanotechnol. **2**, 114 (2007).
[10] F. L. Walls and J. J. Gagnepain, IEEE Trans. Ultrason. Ferroelectr. Freq. Control **39**, 241 (1992).
[11] T. Thundat, G. Y. Chen, R. J. Warmack, D. P. Allison, and E. A. Wachter, Anal. Chem. **67**, 519 (1995).
[12] W. Y. Shih, Q. Zhu, and W. H. Shih, J. Appl. Phys. **104**, 074503 (2008).
[13] E. P. Quevy and R. T. Howe, Proceedings of the IEEE Radio Frequency Integrated Circuits (RFIC) Symposium, Long Beach, CA, 2005, pp. 113–116.
[14] J. J. Caron, R. B. Haskell, P. Benoit, and J. F. Vetelino, IEEE Trans. Ultrason. Ferroelectr. Freq. Control **45**, 1393 (1998).
[15] T. Ono, D. F. Wang, and M. Esashi, Proceedings of the IEEE Conference on Sensors, Toronto, ON, 2003, Vol. 2, pp. 825–829.
[16] K. Sundaresan, G. K. Ho, S. Pourkamali, and F. Ayazi, IEEE J. Solid-State Circuits **42**, 1425 (2007).
[17] J. H. Seo, K. S. Demirci, A. Byun, S. Truax, and O. Brand, J. Appl. Phys. **104**, 014911 (2008).
[18] R. Melamud, B. Kim, S. A. Chandorkar, M. A. Hopcroft, M. Agarwal, C. M. Jha, and T. W. Kenny, Appl. Phys. Lett. **90**, 244107 (2007).
[19] W. Pang, R. C. Ruby, R. Parker, P. W. Fisher, M. A. Unkrich, and J. D. Larson III, IEEE Electron Device Lett. **29**, 315 (2008).
[20] J. Bjurstrom, G. Wingqvist, V. Yantchev, and I. Katardjiev, J. Micromech. Microeng. **17**, 651 (2007).
[21] W.-T. Hsu, J. R. Clark, and C. T. C. Nguyen, Proceedings of the International Electron Devices Meeting (IEDM), San Francisco, CA, 2000, pp. 399–402.
[22] J. Veris, Sens. Actuators, A **57**, 179 (1996).
[23] R. G. Azevedo, W. Huang, O. M. O'Reilly, and A. P. Pisano, Sens. Actuators, A **144**, 374 (2008).
[24] M. Koskenvuori, V. Kaajakari, T. Mattila, and I. Tittonen, Proceedings of the 21st IEEE International Conference on Micro Electro Mechanical Systems (MEMS), Tucson, AZ, 2008, pp. 78–81.
[25] D. E. Pierce, Y. Kim, and J. R. Vig, IEEE Trans. Ultrason. Ferroelectr. Freq. Control **45**, 1238 (1998).
[26] It is important to note how the terms "mode" and "overtone" are used throughout this work. A mechanical structure can resonate in different classes of modes (or simply, modes), e.g., flexural, torsional, or longitudinal modes. Meanwhile, each class of modes consists of overtones, which correspond to the eigenvalues of the general solution for the governing resonance equation of that particular mode class (e.g., flexural modes or overtones).
[27] S. Timoshenko, D. H. Young, and W. Weaver, *Vibration Problems in Engineering*, 4th ed. (Wiley, New York, 1974).
[28] N. Lobontiu, *Dynamics of Microelectromechanical Systems*, 1st ed. (Springer, New York, 2007).
[29] A. Hierlemann, O. Brand, C. Hagleitner, and H. Baltes, Proc. IEEE **91**, 839 (2003).
[30] N. V. Lavrik, M. J. Sepaniak, and P. G. Datskos, Rev. Sci. Instrum. **75**, 2229 (2004).
[31] P. M. Morse, *Vibration and Sound*, 2nd ed. (McGraw-Hill, New York, 1948).
[32] H. J. Butt and M. Jaschke, Nanotechnology **6**, 1 (1995).
[33] R. A. Johnson, *Mechanical Filters in Electronics* (Wiley, New York, 1983).
[34] S. Dohn, R. Sandberg, W. Svendsen, and A. Boisen, Appl. Phys. Lett. **86**, 233501 (2005).
[35] S. Dohn, W. Svendsen, A. Boisen, and O. Hansen, Rev. Sci. Instrum. **78**, 103303 (2007).
[36] K. Naeli and O. Brand, Rev. Sci. Instrum. **80**, 045105 (2009).